

Sejkora *et al.* Škáchaite, a new member of the dolomite group

Škáchaite, $\text{CaCo}(\text{CO}_3)_2$, a new member of the dolomite group, from the Brod deposit near Příbram, Czech Republic

JIŘÍ SEJKORA^{1*}, JAKUB PLÁŠIL², ZDENĚK DOLNÍČEK¹, JANA ULMANOVÁ¹ AND RADEK ŠKODA³

¹Department of Mineralogy and Petrology, National Museum, Cirkusová 1740, 193 00 Praha 9, Czech Republic

²Institute of Physics of the CAS, Na Slovance 1999/2, 182 21 Praha 8, Czech Republic

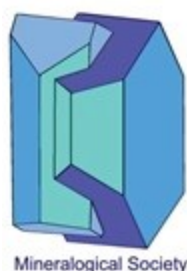
³Department of Geological Sciences, Faculty of Science, Masaryk University, Kotlářská 2, 611 37 Brno, Czech Republic

Author for correspondence: Jiří Sejkora, Email: jiri.sejkora@nm.cz

Received xx xx 2023, ...

Abstract

Škáchaite (IMA 2022-143) is a new mineral species discovered in samples from the hydrothermal vein B117, shaft No. 6 at the Brod deposit of the uranium and base-metal Příbram ore district, central Bohemia, Czech Republic. Škáchaite forms anhedral grains up to 50 μm in size and 20-100 μm thick growth zones in škáchaite-dolomite crystals as a part of carbonate (dolomite, calcite, siderite, spherocobaltite, ankerite, kutnohorite, minrecordite) gangue, associated with native silver, sulfides and arsenides. Škáchaite is pale to bright pink with vitreous luster. The Mohs hardness is *ca.* 3½-4, similar to other members of the dolomite group. The calculated density is 3.140 $\text{g}\cdot\text{cm}^{-3}$. Škáchaite is optically uniaxial negative; the indices of refraction are $\omega = 1.741(3)$ and $\varepsilon = 1.535(3)$. Based on electron-microprobe analyses, its empirical formula is $\text{Ca}_{1.00}(\text{Co}_{0.45}\text{Mg}_{0.38}\text{Ca}_{0.08}\text{Fe}_{0.05}\text{Mn}_{0.03}\text{Zn}_{0.01})_{\Sigma 1.00}(\text{CO}_3)_2$. The ideal formula is $\text{CaCo}(\text{CO}_3)_2$, which requires (in wt%) CaO 25.60, CoO 34.21, CO₂ 40.19, a total of 100.00. Škáchaite is trigonal, *R*-3, with unit-cell parameters $a = 4.8177(18)$, $c = 16.093(7)$ Å, $V = 323.5(2)$ Å³, $Z = 3$. The strongest reflections of the calculated X-ray powder diffraction pattern [$d(\text{Å})/I_{\text{rel}}/(hkl)$] are: 3.704/13/(10-2), 2.896/100/(104), 2.409/15/(110), 2.019/17/(202), 1.812/19/(10-8), 1.792/16/(11-6). According to the single-crystal X-ray diffraction data ($R_1 = 0.0304$ for 94 reflections with $[I > 3\sigma(I)]$), the crystal structure of škáchaite is isotypic with its Mg-analogue, dolomite. The Raman spectrum of škáchaite, as well as the tentative assignment of observed bands, are given in this paper. The mineral is



This is a 'preproof' accepted article for Mineralogical Magazine. This version may be subject to change during the production process.

DOI: 10.1180/mgm.2024.21

named in honor of Pavel Škácha, a Czech mineralogist and curator of the mineralogical collection of the Mining Museum Příbram, Czech Republic.

Key-words: škáchaite; new mineral; carbonate; cobalt; dolomite group; crystal structure; Brod deposit; Příbram ore area; Czech Republic.

Introduction

During our long-term systematic mineralogical research on the Příbram ore area in the Czech Republic (Sejkora *et al.*, 2021, 2022; Škácha *et al.*, 2017, 2018, 2021; Dolníček *et al.*, 2023), we also focused attention on the study of the unique bonanza-type silver mineralization of the hydrothermal vein B117 of the Brod deposit. As part of this research, we identified a new species, a Co-dominant member of the dolomite group. In this paper, we report its description.

The new mineral is named škáchaite in honor of Pavel Škácha (born 1981), a Czech mineralogist and curator of the mineralogical collection of the Mining Museum Příbram, Czech Republic. Pavel Škácha is the author of over sixty publications in the field of mineralogy and the history of mining, including the description of more than twelve new mineral species, especially from the Příbram ore area and from the Jáchymov ore district (Czech Republic). The new mineral and its name were approved by the Commission on New Minerals, Nomenclature and Classification of the International Mineralogical Association (IMA 2022-143). Its mineral symbol, in accordance with Warr (2021), is Škác. Holotype material (polished section) of škáchaite is deposited in the collections of the Department of Mineralogy and Petrology, National Museum in Prague, Cirkusová 1740, 193 00 Praha 9, Czech Republic, under the catalog number P1P 52/2022. This polished section was taken from a large sample deposited in the same collection under catalog number P1N 49.308. Another polished section (cotype) is deposited in the collection of the Mining Museum Příbram, Czech Republic (catalog number 1/2024).

Occurrence and mineral description

Occurrence

Škáchaite has been found in samples from the hydrothermal vein B117 between the 5th-6th level (depth 250-300 m below surface) of shaft No. 6 - Brod southeast of Příbram. In the period 1950-1991, this mine was one of the shafts opening the shallow parts of the Brod deposit, which belongs to the uranium and base-metal Příbram ore district, central Bohemia, Czech Republic (Komínek, 1995). The GPS coordinates of occurrence of škáchaite are 49°40'5.094"N, 14°1'13.809"E. The uranium and base-metal Příbram ore district and the neighboring Březové Hory ore district form the two main parts of the Příbram ore area.

The Příbram uranium and base-metal district represents the most significant accumulation of vein-type hydrothermal U ores in the Czech Republic. The hydrothermal U-mineralization of late Variscan age is related to a 1–2 km wide and almost 25 km long zone formed by strongly tectonized series of Upper Proterozoic sedimentary rocks along the contact with granitoids of the Devonian-Carboniferous Central Bohemian Plutonic Complex

(Litochleb *et al.*, 2003). For instance, the complete list of over 320 minerals identified to date from this area is given on mindat.org at <http://www.mindat.org/loc-779.html>.

The holotype polished section of the new mineral was taken from a museum specimen (National Museum Prague, catalog number P1N 49.308) with dimensions $45 \times 42 \times 13$ cm, which represents the complete profile through a 22 cm thick symmetrical vein filling, including also surrounding rock (Fig. 1). This unique sample of bonanza-type silver mineralization contains abundant elongated native silver aggregates up to 6 cm in length in gangue formed by various types of carbonates - calcite, siderite, spherocobaltite, ankerite, kutnohorite, minrecordite and members of series dolomite - škáchaite. Other associated minerals are safflorite, löllingite, cobaltpentlandite, Co-analogue of heazlewoodite, siegenite, carrollite, mckinstryite, jalpaite, chalcocite, tetrahedrite-(Zn), argentotetrahedrite-(Fe), not yet approved *argentotennantite-(Fe)* (IMA 2023-126 under voting), hematite, sphalerite, galena, chalcopyrite, pyrite and hisingerite (Litochleb *et al.*, 2002). Škáchaite is of the low-temperature hydrothermal origin.

Physical and optical properties

Škáchaite occurs as anhedral grains up to 50 μm in size and growth zones in škáchaite-dolomite zoned crystals (Fig. 2) with thickness up to 100 μm but usually only 5-20 μm . Škáchaite is pale to bright pink in colour; tiny fragments are translucent. The mineral has a white streak and vitreous luster. It does not fluoresce under either short- or long-wave ultraviolet light. The mineral is brittle, cleavage on $\{10\text{-}11\}$ is perfect; the Mohs hardness cannot be measured due to size of škáchaite grains and may be close to $3\frac{1}{2}$ -4, similar to other members of the dolomite group. The density could not be measured directly because of the small amount of available material. The calculated density is 3.140 g/cm^3 based on the empirical formula and unit-cell volume from single-crystal data.

In thin section, škáchaite is pink with a distinct rhombohedral cleavage. It is optically uniaxial negative, with $\omega = 1.741(3)$, $\varepsilon = 1.535(3)$ (measured at 589 nm). Škáchaite is not pleochroic and has hints of undulatory extinction. The Gladstone-Dale compatibility index, $1 - (K_P/K_C)$, is -0.050 for the empirical formula and unit-cell parameters from single-crystal data, indicating good compatibility (Mandarino, 1981).

Chemical composition

Chemical analyses were performed using a Cameca SX100 electron microprobe operating in wavelength-dispersive mode (15 kV, 10 nA and 3 μm beam size). The following standards and X-ray lines were used to minimize line overlaps: Co ($\text{CoK}\alpha$), diopside ($\text{MgK}\alpha$), hematite ($\text{FeK}\alpha$), rhodonite ($\text{MnK}\alpha$), wollastonite ($\text{CaK}\alpha$) and ZnO ($\text{ZnK}\alpha$). Peak counting times were 20 s for all elements, and 10 s for each background. Contents of other measured elements (Al, Ba, Cu, Na, Ni, P, Pb, Si, Sr) were always below detection limits. Matrix correction by PAP algorithm (Pouchou and Pichoir, 1985) was applied to the data (measured oxides and calculated amount of CO_2 resting to analytical sum of 100 wt%). Carbonate content could not be analyzed directly because of the minute amount of material available; it was confirmed by Raman spectroscopy and single crystal-structure study and calculated by stoichiometry based on the ideal content of two CO_3 groups in the crystal structure of dolomite group minerals.

Table 1 gives the chemical composition (mean of eleven analyses) of the škáchaite grain used for the single-crystal study (holotype polished section). Individual point analyses (Table S1) show Co-dominant character (0.41-0.49 *apfu*) with contents of Mg (0.35-0.41 *apfu*) and minor Fe (0.04-0.06 *apfu*), Mn (0.03-0.05 *apfu*) and Zn (up to 0.01 *apfu*). On the basis $\Sigma\text{cations} = 2$ atoms per formula unit (*apfu*), the average empirical formula is $\text{Ca}_{1.00}(\text{Co}_{0.45}\text{Mg}_{0.38}\text{Ca}_{0.08}\text{Fe}_{0.05}\text{Mn}_{0.03}\text{Zn}_{0.01})_{\Sigma 1.00}(\text{CO}_3)_2$. The ideal formula is $\text{CaCo}(\text{CO}_3)_2$, which requires (in wt%) CaO 25.60, CoO 34.21, CO₂ 40.19, a total 100.00.

Škáchaite was also determined in other 26 polished sections (taken from the same museum sample) usually in forms thin (units to tens μm) zones in škáchaite-dolomite grains. In the chemical analyses (Table S2), the predominant Co (0.35-0.59 *apfu*) is accompanied by Mg (0.17-0.44 *apfu*), Fe (0.03-0.31 *apfu*), Mn (0.01-0.12 *apfu*) and minor Ni and Zn up to 0.06 and 0.03 *apfu*, respectively.

Raman spectroscopy

The Raman spectra of škáchaite were collected in the range 50-4000 cm^{-1} using a DXR dispersive Raman Spectrometer (Thermo Scientific) mounted on a confocal Olympus microscope. The Raman signal was excited by an unpolarised red 633 nm He-Ne gas laser and detected by a CCD detector. The experimental parameters were: 100x objective, 10 s exposure time, 100 exposures, 50 μm pinhole spectrograph aperture and 8 mW laser power level. The eventual thermal damage of the measured points was excluded by visual inspection of the excited surface after measurement, observation of possible decay of spectral features at the start of excitation, and checking for thermal downshift of Raman lines. The instrument was set up by a software-controlled calibration procedure using multiple neon emission lines (wavelength calibration), multiple polystyrene Raman bands (laser frequency calibration) and standardized white-light sources (intensity calibration). Spectral manipulations were performed using the Omnic 9 software (Thermo Scientific).

The Raman spectrum of škáchaite is given in Figure 3. The main bands observed are (in wavenumbers): 1748, 1437, 1094, 723, 294 and 173 cm^{-1} . The experimental spectrum of škáchaite agrees very well with published Raman spectra of dolomite (e.g., Gillet *et al.*, 1993; Perrin *et al.*, 2016). The strong band at 1094 cm^{-1} is attributed to the symmetric stretching vibration (ν_1) and the band at 1437 cm^{-1} to the asymmetric stretching vibration (ν_3) of $(\text{CO}_3)^{2-}$ groups. A band at 723 cm^{-1} is assigned to the in-plane bending vibration (ν_4). The out-of-plane bending vibration (ν_2) is inactive in the Raman spectrum, while its overtone ($2\nu_2$) is observed at 1748 cm^{-1} . The bands below 300 cm^{-1} (294 and 173 cm^{-1}) are attributed to lattice modes.

X-ray diffraction data

Single-crystal X-ray studies were carried out on a thin growth zone retrieved from a larger fragment identified by WDS, which was selected to be tested on a Rigaku SuperNova single-crystal diffractometer equipped with the Atlas S2 CCD detector (microfocused $\text{MoK}\alpha$ radiation). The approximate dimensions of the fragment are $0.06 \times 0.01 \times 0.01$ mm and the diffraction experiment yielded the following data: trigonal space group $R\bar{3}$ (no. 148), $a = 4.8177(18)$, $c = 16.093(7)$ Å, $V = 323.5(2)$ Å³, $Z = 3$. The $c:a$ ratio calculated from unit-cell

parameters is 3.3404. The intensity data for škáchaite were processed using the Rigaku CrysAlis package, including applying an empirical multi-scan absorption correction (Rigaku, 2019). The structure was solved using the intrinsic phasing algorithm of the SHELXT program (Sheldrick, 2015). Refinement proceeded by full-matrix least-squares on F^2 using Jana2020 (Petříček *et al.*, 2023). A reverse-obverse twinning (Table 2) was taken into account during the refinement in Jana (see Petříček *et al.*, 2016). The anisotropic structural model converged to $R_1 = 0.0304$ for 94 reflections with $F_o > 3\sigma(F_o)$ for 20 refined parameters, including site-occupancy refinement for Mg/Co. The final refinement returned site occupancies of $\text{Co}_{0.503}$ and $\text{Mg}_{0.497}$; the corresponding site scattering $19.5e^-$ is in line with those obtained from the WDS ($20.7e^-$). Details of data collection and refinement are given in Table 2. Fractional atomic coordinates and equivalent isotropic displacement parameters are reported in Table 3 and selected bond-distances and polyhedral volumes in Table 4. Anisotropic displacement parameters are reported in the crystallographic information file (CIF) deposited with the Principal Editor of Mineralogical Magazine and available as Supplementary material (see below).

Powder X-ray diffraction data could not be collected due to the paucity of available material. The experimental pseudo-Gandolfi scan was attempted to be collected, but the observed intensities were extremely weak. This is most probably due to small volume of diffracting material (see the crystal dimensions). Consequently, powder X-ray diffraction data, given in Table 5, were calculated using the software *PowderCell* 2.3 (Kraus and Nolze, 1996) based on the structural model given in Tables 2 and 3.

Crystal structure of škáchaite

Crystal structure of škáchaite is proven (as expected) to be isotopic with dolomite. The study of Perchiazzi *et al.* (2018) based on samples from Tenke-Fungurume district, Democratic Republic of Congo, documented the then maximum Co substitution for Mg in dolomite corresponding to the formula $\text{Ca}(\text{Mg}_{0.70}\text{Co}_{0.30})(\text{CO}_3)_2$ (crystal named CD6). The crystal fragment (Fig. 2) investigated in the current study yielded the composition $\text{Ca}(\text{Co}_{0.503}\text{Mg}_{0.497})(\text{CO}_3)_2$ (and further WDS analyses have proven even more Co for some of the points measured - up to 0.59 apfu). A comparison of selected polyhedral measures and interatomic distances is given in Tables 4, 6-7. With the increasing Co-content in the dolomite-group minerals, both the unit-cell parameters increase as well, with substantial increments in a as well as in c parameters (Figs. 4 and 5). As has been already pointed out and discussed by Perchiazzi *et al.* (2018) the AO_6 octahedron is always larger than the corresponding BO_6 octahedron. Increasing the Co content, the B–O bond length ($2.107(5) \text{ \AA}$ for škáchaite) and BO_6 polyhedral volume ($12.46(1) \text{ \AA}^3$ for škáchaite) both increase, whereas the opposite behavior is apparent for the AO_6 polyhedron (Table 4). Perchiazzi *et al.* (2018) also pointed out that with increasing Co content, the AO_6 and BO_6 octahedra behave distinctly: the AO_6 octahedron shrinks anisotropically through the shortening of its basal edges, leading to the meager increase of the a cell parameter. The BO_6 octahedron instead expands, stretching both its “basal” and “lateral” edges (Table 6). The explanation for the anisotropic expansion of unit-cell parameters of all up-to-date known “Co-dolomites” (including škáchaite as well) is caused by the anisotropic variation of AO_6 and BO_6

polyhedral volumes, coupled with the presence of rigid CO₃ groups lying in the (0001) plane (Perchiazzi *et al.*, 2018).

Discussion

Cobalt mineralogy is dominated by S and As bearing minerals, both of primary or supergene origin (Hazen *et al.*, 2017). Škáchaite is only the second anhydrous Co carbonate mineral to be defined after spherocobaltite; other four known Co carbonates, comblainite, kaznakhtite, kolwezite and perchiazziite, contain hydroxyl groups or water.

Cobalt-containing dolomites were described from several occurrences in the Central African Copperbelt (Deliens and Piret, 1980; Fay and Barton, 2012; Van Langendonck *et al.*, 2013). Their chemical composition was studied by EDS analyses (Douglass 1992 and 1999; Gauthier and Deliens, 1999), which found Co contents in B site not exceeding 0.11 - 0.18 *apfu*. Sweeney *et al.* (1986) state that samples from Konkola Basin in Zambia have up to 0.08 *apfu* Co. Minceva-Stefanova (1997) reported an EPMA study performed on strongly zoned Co-rich dolomite crystals from an unknown locality with Co contents up to 0.35 *apfu*. A crystallographic study of cobalt-rich dolomite from Kolwezi (Democratic Republic of Congo) was performed by Perchiazzi (2015), who reported its chemical data with 0.17 *apfu* Co based on EDS data, only. A complete genetic, geochemical, and mineralogical study of Co-rich carbonates from the Tenke-Fungurume District, Democratic Republic of Congo, was published by Barton *et al.* (2014), the maximum observed Co content is 0.30 *apfu*; the same material was used for single crystal structural studies (Perchiazzi *et al.*, 2018).

The observed Co contents in the samples from the Brod deposit (Fig. 6) are significantly higher than those published so far (Fig. 7). We found thin (tens μm) zones with contents up to 0.59 *apfu* Co. The grain extracted for single-crystal X-ray diffraction shows contents 0.41-0.49 *apfu* Co; cobalt always prevails over Mg (Fig. 6).

The Figures 4 and 5 show that the unit-cell parameters of Co-rich dolomites and škáchaite expand with increasing Co content; the discrepancy of sample from Kolwezi (Perchiazzi, 2015) could be explained by the Mg/Co ratio only being measured by EDS; by the presence of a fine undetected chemical zoning; by unrecognized contamination by mineral inclusion(s) in the analysed volume; or by an error introduced by twinning on the unit-cell determination (Perchiazzi *et al.*, 2018).

Conclusion

Škáchaite is a new Ca-Co dominant member of the dolomite group (Table 8) together with ankerite (Ca-Fe), dolomite (Ca-Mg), kutnohorite (Ca-Mn), minrecordite (Ca-Zn) and norsethite (Ba-Mg); Strunz Class 5.AB.10. It does not correspond to any valid or invalid unnamed mineral (Smith and Nickel, 2007).

Škáchaite discovery and its comparison with previously known Co-containing dolomites confirm the fundamental role played by the investigation of natural mineral assemblages to reveal the possibilities of contents of elements such as Co in the crystal structure of dolomite-group minerals. In the past, it has been reported "Cobalt does not form a stable dolomite-structured carbonate, either with other transition metal ions or with Ca²⁺" (Reeder, 1983; Barton *et al.*, 2014) and Co-dominant dolomite was so far not obtained in

synthetic runs (e.g., Goldsmith and Northrop, 1965; Rosenberg and Foit, 1979).

Supplementary material. To view supplementary material for this article, please visit ...

Acknowledgments: The helpful comments of an anonymous reviewer, Peter Leverett, Christian L. Lengauer, associated editor Owen Missen and principal editor Stuart Mills are greatly appreciated. The study was financially supported by the Ministry of Culture of the Czech Republic (long-term project DKRVO 2024-2028/1.II.a; National Museum, 00023272) and the Czech Science Foundation (project 19-16218S) for JS, ZD and JU. We acknowledge CzechNanoLab Research Infrastructure supported by MEYS CR (LM2023051) for the financial support of the data collection.

Competing interests. The author declare none.

References

- Barton, I. F., Yang, H. and Barton, M. D. (2014) The mineralogy, geochemistry, and metallurgy of cobalt in the rhombohedral carbonates. *The Canadian Mineralogist*, **52**, 653-670.
- Deliens, M. and Piret, P. (1980) La kolwesite, un hydrocarbonate de cuivre et de cobalt analogue a la glaukosphaerite et a la rosasite. *Bulletin de Mineralogie*, **103**(2), 179-184.
- Dolníček, Z., Ulmanová, J., Sejkora, J., Knížek, F. and Škácha, P. (2023) Mineralogy and genesis of the Pb-Zn-Sb-Ag vein H32A in the Příbram uranium and base-metal district, Bohemian Massif, Czech Republic. *Ore Geology Reviews*, **162**, 105695.
- Douglass, D.L. (1992) Cobaltoan Calcite = Cobaltoan Dolomite. *Mineralogical Record*, **23**, 445-446.
- Douglass, D. L. (1999) Cobaltoan calcites and dolomites from Katanga. *Mineralogical Record*, **30**, 269-273.
- Fay, I. and Barton, M. D. (2012) Alteration and ore distribution in the Proterozoic Mines Series, Tenke-Fungurume Cu-Co district, Democratic Republic of Congo. *Mineralium Deposita*, **47**(5), 501-519.
- Garavelli, C.G., Vurro, F. and Fioravanti, G.C. (1982) Minrecordite a new mineral from Tsumeb. *The Mineralogical Record*, **13**, 131-136.
- Gauthier, G. and Deliens, M. (1999) Cobalt minerals of the Katanga Crescent, Congo. *Mineralogical Record*, **30**, 255-267.
- Gillet, P., Biellmann, C., Reynard, B. and McMillan, P. (1993) Raman spectroscopic studies of carbonates Part I: High-pressure and high-temperature behaviour of calcite, magnesite, dolomite and aragonite. *Physics and Chemistry of Minerals*, **20**(1), 1-18.
- Goldsmith, J.R. and Northrop, D.A. (1965) Subsolidus phase relations in the systems CaCO₃-MgCO₃-CoCO₃ and CaCO₃-MgCO₃-NiCO₃. *The Journal of Geology* **73**(6), 817-829.
- Hazen, R.M., Hystad, G., Golden, J.J., Hummer, D.R., Liu, C., Downs, R.T., Morrison S.M., Ralph, J. and Grew, E. S. (2017) Cobalt mineral ecology. *American Mineralogist*, **102**(1), 108-116.

- Komínek, J. (1995) *Geology of the wide surroundings and of the deposit, part I and II. Final report on the uranium district Příbram*. MS DIAMO, Příbram, 418 p. (in Czech)
- Kraus, W. and Nolze, G. (1996) POWDER CELL – a program for the representation and manipulation of crystal structures and calculation of the resulting X-ray powder patterns. *Journal of Applied Crystallography*, **29**, 301-303.
- Litochleb, J., Sejkora, J. and Šrein, V. (2002) Mineralogy of silver mineralization from Brod near Příbram (the Příbram uranium - polymetallic district, central Bohemia, Czech Republic). *Bulletin mineralogicko-petrologického oddělení Národního muzea v Praze*, **10**, 221-234. (in Czech)
- Litochleb, J., Černý, P., Litochlebová, E., Sejkora, J. and Šreinová, B. (2003) The deposits and occurrences of mineral raw materials in the Střední Brdy Mts. and the Brdy piedmont area (Central Bohemia). *Bulletin mineralogicko-petrologického oddělení Národního muzea v Praze*, **11**, 57–86 (in Czech)
- Mandarino, J.A. (1981) The Gladstone-Dale relationship: Part IV. The compatibility concept and its application. *The Canadian Mineralogist* **19**, 441-450.
- Minceva-Stefanova, J. (1997) First finding of high miscibility in the system $\text{CaMg}(\text{CO}_3)_2$ – $\text{CaCo}(\text{CO}_3)_2$ in nature. *Geochemistry, Mineralogy and Petrology*, **32**, 5-16.
- Peacor, D.R., Essene, E.J. and Gaines, A.M. (1987) Petrologic and crystal-chemical implications of cation order-disorder in kutnahorite ($\text{CaMn}(\text{CO}_3)_2$). *American Mineralogist*, **72**, 319-328.
- Perchiazzi, N. (2015) Crystal structure study of a cobaltoan dolomite from Kolwezi, Democratic Republic of Congo. *Acta Crystallographica Section E: Crystallographic Communications*, **71**(3), i3-i3
- Perchiazzi, N., Barton, I. F. and Vignola, P. (2018) Incorporation of Co in the dolomite structure: coupled EPMA and single crystal structural studies of Co-rich dolomite from the Tenke-Fungurume district, Democratic Republic of Congo. *The Canadian Mineralogist*, **56**(2), 151-158
- Perrin, J., Vielzeuf, D., Laporte, D., Ricolleau, A., Rossman, G.R. and Floquet, N. (2016) Raman characterization of synthetic magnesian calcites. *American Mineralogist*, **101**(11), 2525-2538.
- Pertlik, F. (1986) Structures of hydrothermally synthesized cobalt(II) carbonate and nickel(II) carbonate. *Acta Crystallographica*, **C42**, 4–5.
- Petříček, V., Dušek, M., Plášil, J. (2016) Crystallographic computing system Jana2006: solution and refinement of twinned structures. *Zeitschrift für Kristallographie*, **231**(10), 583–599.
- Petříček, V., Palatinus, L., Plášil, J. and Dušek, M. (2023) Jana2020 – a new version of the crystallographic computing system Jana. *Zeitschrift für Kristallographie*, **238**(7–8), 271–282.
- Pouchou, J.L. and Pichoir, F. (1985) “PAP” ($\phi\rho Z$) procedure for improved quantitative microanalysis. Pp. 104-106 in: *Microbeam Analysis* (J.T. Armstrong, editor). San Francisco Press, San Francisco.
- Rigaku (2019) CrysAlis CCD and CrysAlis RED. Rigaku- Oxford Diffraction Ltd, Yarnton, Oxfordshire, UK.

- Reeder, R.J. (1983) Crystal chemistry of the rhombohedral carbonates. *In Carbonates: Mineralogy and Chemistry* (R.J. Reeder, ed.). *Reviews in Mineralogy and Geochemistry*, **11**, 1-47.
- Reeder, R.J. and Dollase, W.A. (1989) Structural variation in the dolomite-ankerite solid-solution series: An X-ray, Moessbauer, and TEM study. *American Mineralogist*, **74**, 1159-1167.
- Rosenberg, P.E. and Foit Jr, F.F. (1979). The stability of transition metal dolomites in carbonate systems: a discussion. *Geochimica et Cosmochimica Acta*, **43**(7), 951-955.
- Sejkora, J., Škácha, P., Plášil, J., Dolníček, Z. and Ulmanová, J. (2021) Hrabákite, Ni₉PbSbS₈, a new member of the hauchecornite group from Příbram, Czech Republic. *Mineralogical Magazine*, **85**(2), 189-196.
- Sejkora, J., Dolníček, Z., Zachariáš, J., Ulmanová, J., Šrein, V. and Škácha, P. (2022) Mineralogical and fluid inclusion evidence for reworking of Au(-Bi) mineralization by Ag-Sb-base metal-rich fluids from the Bytíz deposit, Příbram uranium and base-metal ore district, Czech Republic. *Minerals*, **12**(12), 1539.
- Sheldrick, G.M. (2015) Crystal structure refinement with SHELXL. *Acta Crystallographica*, **C71**, 3-8.
- Škácha, P., Sejkora, J. and Plášil, J. (2017) Selenide mineralization in the Příbram uranium and base-metal district (Czech Republic). *Minerals*, **7**(6), 91.
- Škácha, P., Sejkora, J. and Plášil, J. (2018) Bytízite, a new Cu-Sb selenide from Příbram, Czech Republic. *Mineralogical Magazine*, **82**(1), 199-209.
- Škácha, P., Sejkora, J., Plášil, J., Dolníček, Z. and Ulmanová, J. (2021) Grimmite, NiCo₂S₄, a new thiospinel from Příbram, Czech Republic. *European Journal of Mineralogy*, **33**(2), 175-187.
- Smith, D.G.W. and Nickel, E.H. (2007) A system for codification for unnamed minerals: report of the Subcommittee for Unnamed Minerals of the IMA Commission on New Minerals, Nomenclature and Classification. *The Canadian Mineralogist*, **45**, 983-1055.
- Sweeney, M., Turner, P. and Vaughan, D.J. (1986) Stable isotope and geochemical studies of the role of early diagenesis in ore formation, Konkola Basin, Zambian Copper Belt. *Economic Geology*, **81**, 1838–1852.
- Van Langendonck, S., Muchez, P., Dewaele, S., Kalubi, A. J. and Cailteux, J.A (2013) Petrographic and mineralogical study of the sediment-hosted Cu-Co ore deposit at Kambove West in the central part of the Katanga Copperbelt (DRC). *Geologica Belgica*, **16**, 91-104.
- Warr, L.N. (2021) IMA-CNMNC approved mineral symbols. *Mineralogical Magazine*, **85**, 291-320.

Table 1. Chemical composition (in wt %) of škáchaite

Element	Mean	Range	S.D.
CaO	29.59	28.78-30.28	0.42
FeO	1.61	1.27-2.09	0.23
MgO	7.55	6.83-8.14	0.41
CoO	16.32	15.17-17.56	0.69
MnO	1.19	0.89-1.54	0.19
ZnO	0.23	0.00-0.42	0.12
CO ₂ *	42.90	42.21-43.34	0.34
Total	99.39		

* CO₂ content was calculated based on two CO₃ groups present in the crystal structure of dolomite-group minerals.

Table 2. Crystal data and refinement details for škáchaite.

Formula derived from refinement	Ca(Co _{0.503} Mg _{0.497})(CO ₃) ₂
Unit-cell parameters	
<i>a</i> [Å]	4.8177(18)
<i>c</i> [Å]	16.093(7)
<i>V</i> [Å ³]	323.5(2)
<i>Z</i>	3
Space group	<i>R</i> -3
<i>D</i> _{calc} (g cm ⁻³)	3.108
Temperature	296 K
Wavelength	MoKα, 0.71073 Å
Crystal dimensions	0.061 × 0.014 × 0.013 mm
Collection mode	ω scans to fill an Ewald sphere
Frame width, counting time	1.0, 400 s
Limiting θ angles; completeness to θ _{max}	3.80–28.30°; 0.71
Limiting Miller indices	−2 < <i>h</i> < 5, −4 < <i>k</i> < 3, −17 < <i>l</i> < 16
No. of reflections	167
No. of independent reflections	127
No. of observed reflections (criterion)	94 [<i>I</i> > 3σ(<i>I</i>)]
Absorption correction (mm ⁻¹), method	3.35, multi-scan
<i>T</i> _{min} / <i>T</i> _{max}	0.884/1
<i>R</i> _{int}	0.015
<i>F</i> ₀₀₀	298
Refinement by Jana2020 on <i>F</i> ²	
Parameters, constraints, restraints	20, 2, 0
<i>R</i> ₁ , <i>wR</i> ₂ (obs)	0.0304, 0.0375
<i>R</i> ₁ , <i>wR</i> ₂ (all)	0.0418, 0.0437
GOF (obs, all)	0.98, 1.01
Weighting scheme, weights	σ, 1/(σ ² (<i>I</i>) + 0.000004 <i>I</i> ²)
Δρ _{min} , Δρ _{max} (e Å ⁻³)	−0.32, 0.29
Twin fractions 1, 2, 3	0.637(17)/0.031(12)/0.332(12)
Twin matrices 1/2	$\begin{pmatrix} 1 & -1 & 0 \\ 1 & 0 & 0 \\ 0 & 0 & 1 \end{pmatrix}, \begin{pmatrix} 0 & -1 & 0 \\ -1 & 0 & 0 \\ 0 & 0 & 1 \end{pmatrix}$

Table 3. Atom coordinates, equivalent atomic displacement parameters (in Å²) and site-occupancies for škáchaite.

	<i>x</i>	<i>y</i>	<i>z</i>	<i>U</i> _{eq}	Site occupancy	BVS*
A (Ca)	0	0	0	0.0126(7)	Ca _{1.00}	1.91
B (Co,Mg)	0	0	0.5	0.0115(7)	Co _{0.503(10)} Mg _{0.497(10)}	1.96
C	0	0	0.2431(5)	0.0133(18)	C _{1.00}	4.06
O	0.2496 (7)	-0.0304 (8)	0.2442(2)	0.0169(14)	O _{1.00}	2.33

* BVS – sum of the bond-valences (in valence units) incident upon the atomic site

Table 4. Bond-distances (in Å) and polyhedral volumes (in Å³) for škáchaite in comparison with selected members of the dolomite-škáchaite series.

	reference	A*–O (×6)	B*–O (×6)	<i>V</i> _A (Å ³)	<i>V</i> _B (Å ³)
škáchaite	this paper	2.376(3)	2.107(5)	17.82(1)	12.46(1)
CD6	Perchiazzi <i>et al.</i> (2018)	2.3765(9)	2.0970(9)	17.85(1)	12.29(1)
CD1	Perchiazzi <i>et al.</i> (2018)	2.3821(6)	2.0836(6)	17.98(1)	12.05(1)
spherochalcite	Petrlík (1986)		2.110(1)		12.51(1)

Note: CD1 0.00 *apfu* Co, CD6 0.30 *apfu* Co.

*General formula AB(CO₃)₂, where A = Ca and B = Co and Mg

Table 5. Calculated X-ray powder diffraction data for škáchaite. Intensity and d_{hkl} (in Å) were calculated using the software *PowderCell2.3* (Kraus and Nolze, 1996) based on the structural model given in Tables 2 and 3. Only reflections with $I_{\text{calc}} > 1$ are listed. The six strongest reflections are given in bold.

I_{calc}	d_{calc}	hkl
2	5.364	0 0 3
13	3.704	1 0 -2
100	2.896	1 0 4
2	2.682	0 0 6
15	2.409	1 1 0
11	2.197	1 1 -3
10	2.197	1 1 3
17	2.019	2 0 2
7	1.852	2 0 -4
19	1.812	1 0 -8
10	1.792	1 1 6
16	1.792	1 1 -6
3	1.569	2 1 1
4	1.548	1 2 2
8	1.548	2 1 -2
1	1.501	1 0 10
4	1.468	2 1 4
5	1.468	1 2 -4
4	1.448	2 0 8
1	1.436	1 1 -9
2	1.436	1 1 9
1	1.416	2 1 -5
9	1.391	3 0 0
4	1.341	0 0 12

Table 6. “Basal”- and “lateral”-edge dimensions (in Å) of AO₆ (Ca) and BO₆ (Co/Mg) polyhedra in selected members of the dolomite-škáchaite series.

	reference	AO ₆ lateral	AO ₆ basal	BO ₆ lateral	BO ₆ basal
škáchaite	this paper	3.438(6)	3.280(5)	3.018(6)	2.940(8)
CD6	Perchiazzi <i>et al.</i> (2018)	3.4331(13)	3.2871(13)	3.0055(11)	2.9250(14)
CD1	Perchiazzi <i>et al.</i> (2018)	3.4372(10)	3.2990(8)	2.9886(10)	2.9040(10)

Note: CD1 0.00 *apfu* Co, CD6 0.30 *apfu* Co.

Table 7. Geometry of the CO₃ groups in selected members of the dolomite-škáchaite series.

	reference	C–O (×3)	aplanarity
škáchaite	this paper	1.282(5)	0.017(1)
CD6	Perchiazzi <i>et al.</i> (2018)	1.284(1)	0.016(2)
CD1	Perchiazzi <i>et al.</i> (2018)	1.284(1)	0.010(1)

Note: CD1 0.00 *apfu* Co, CD6 0.30 *apfu* Co.

Table 8. Comparison of škáchaite and other Ca-dominant members of the dolomite group.

mineral	škáchaite	dolomite	kutnohorite	ankerite	minrecordite
	this paper	Perchiazzi <i>et al.</i> (2018)	Peacor <i>et al.</i> (1987)	Reeder and Dollase (1989)	Garavelli <i>et al.</i> (1982)
colour	pink	white	pink	white	white
ideal	CaCo(CO ₃) ₂	CaMg(CO ₃) ₂	CaMn(CO ₃) ₂	Ca(Fe ²⁺ ,Mg)(CO ₃) ₂	CaZn(CO ₃) ₂
B _{emp}	Co _{0.45} Mg _{0.38} Ca _{0.08} Fe _{0.05} Mn _{0.03} Zn _{0.01}	Mg _{1.00} Fe _{0.01}	Mn _{0.73} Ca _{0.27}	Fe _{0.68} Mg _{0.27} Mn _{0.05}	Zn _{0.92} Mg _{0.07} Fe _{0.03}
SG	<i>R</i> -3	<i>R</i> -3	<i>R</i> -3	<i>R</i> -3	<i>R</i> -3
<i>a</i> [Å]	4.8177(18)	4.80705(9)	4.894(1)	4.8312(2)	4.8183(4)
<i>c</i> [Å]	16.093(7)	16.0056(4)	16.50(1)	16.1663(3)	16.0295(10)
<i>V</i> [Å ³]	323.5(2)	320.31(1)	342.3(3)	326.77(3)	322.28

note: ideal - ideal formula; B_{emp} - empirical occupation of BO₆ polyhedra ; SG - space group.

Figures

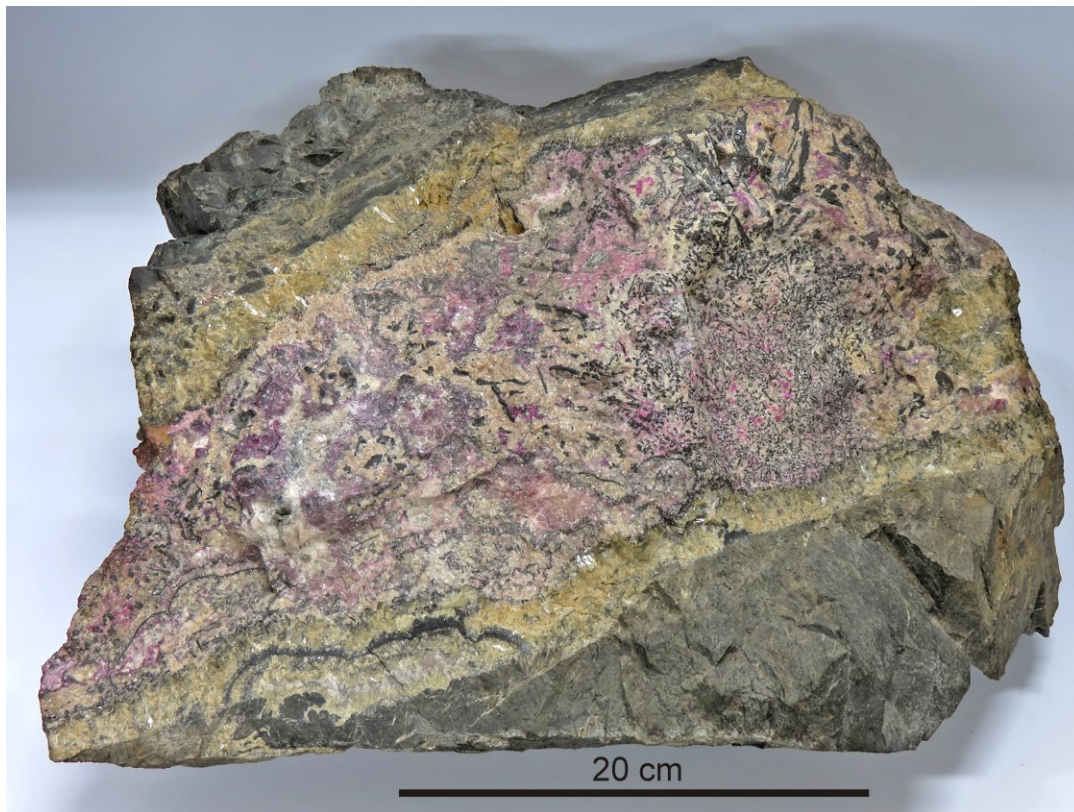


Figure 1. Overall photo of symmetrical vein filling with abundant elongated native silver aggregates up to 6 cm in length in gangue formed by various types of carbonates - calcite, siderite, spherocobaltite, ankerite, kutnohorite, minrecordite and members of series dolomite - škáchaite (catalog number PIN 49.308, mineralogical collection of the National Museum Prague); vein B117, Brod deposit, the uranium and base-metal Příbram ore district (Czech Republic). The holotype of škáchaite was taken from a central part of sample with bright pink carbonate aggregates.

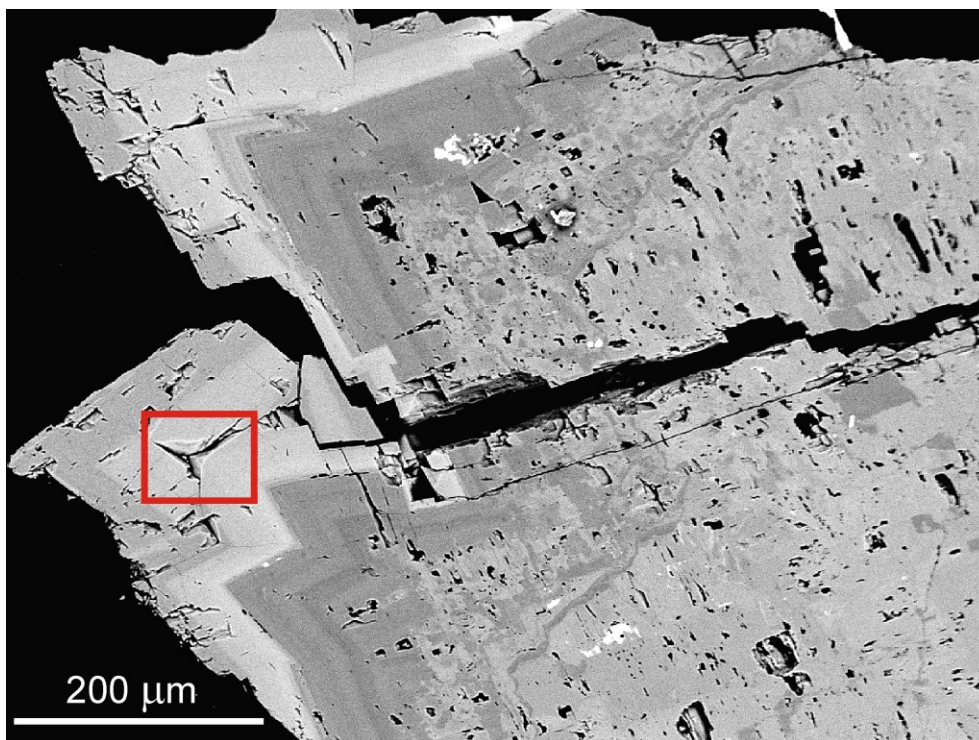


Figure 2. Backscattered electron image of holotype material (P1P 52/2022) - zoned škáchaite-dolomite crystals. Škáchaite zones are white, whereas dolomite (with variable Mg/Co/Fe) ratios) is grey. The red box indicates the area used for the single-crystal X-ray diffraction study.

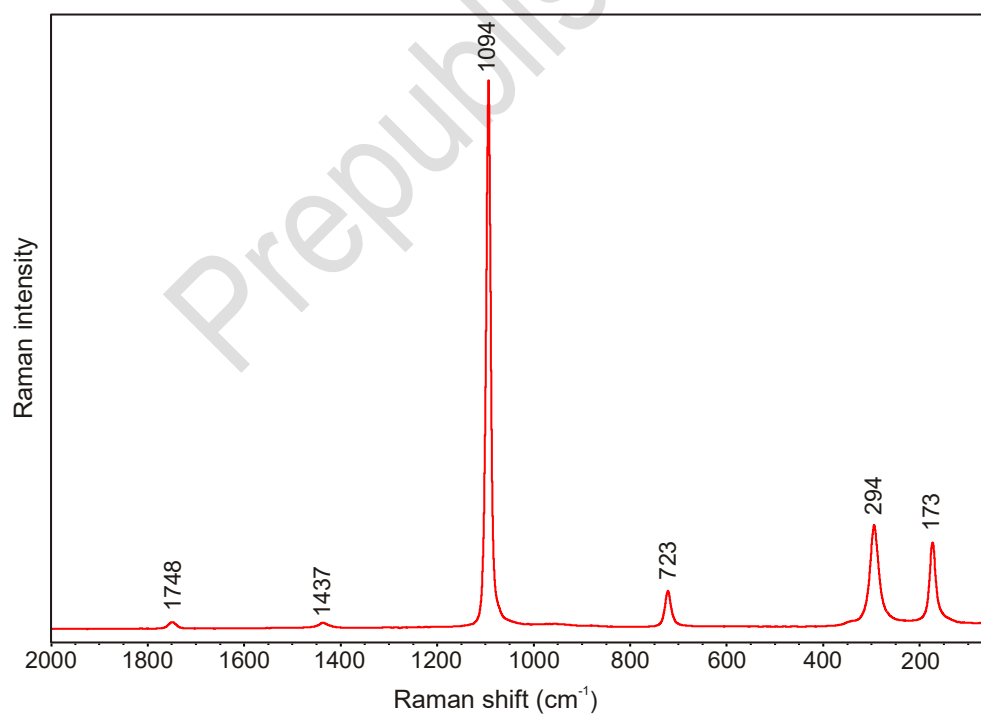


Figure 3. Raman spectrum of škáchaite.

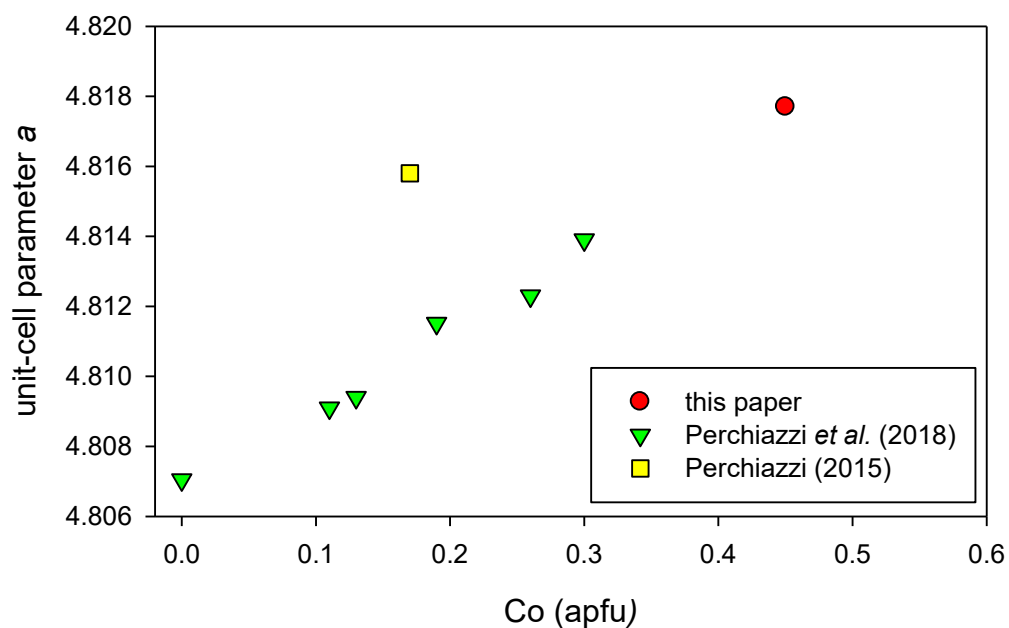


Figure 4. The correlation of unit-cell parameter a (in Å) and Co contents ($apfu$); note: composition published by Perchiazzi (2015) is based on EDS data, only (see remarks in the text).

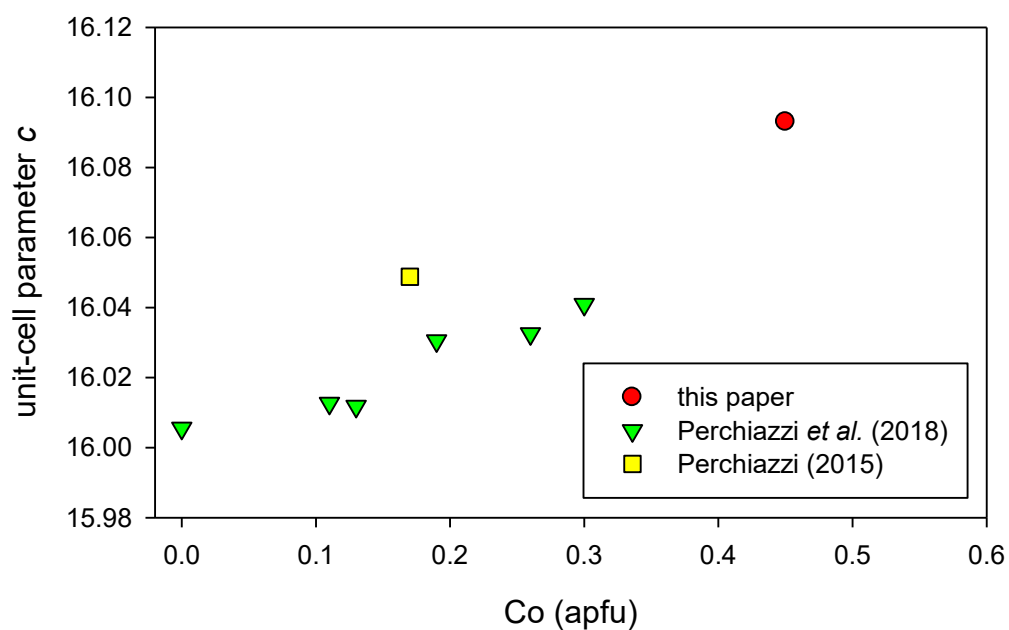


Figure 5. The correlation of unit-cell parameter c (in Å) and Co contents ($apfu$); note: composition published by Perchiazzi (2015) is based on EDS data, only (see remarks in text).

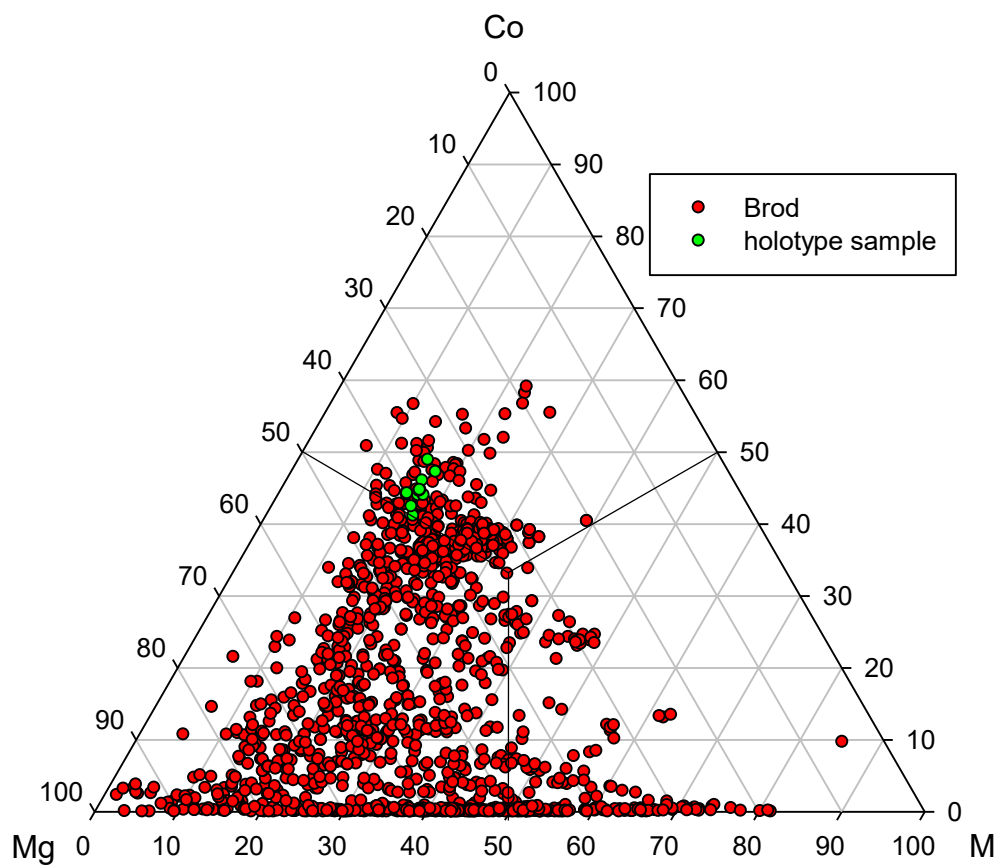


Figure 6. Chemical composition of dolomite-group minerals (about 1400 point analyses) from the hydrothermal vein B117 of the Brod deposit (*unpublished data of authors*) in the Mg-Co-M graph (M = Fe+Mn+Zn+Cu+Ni).

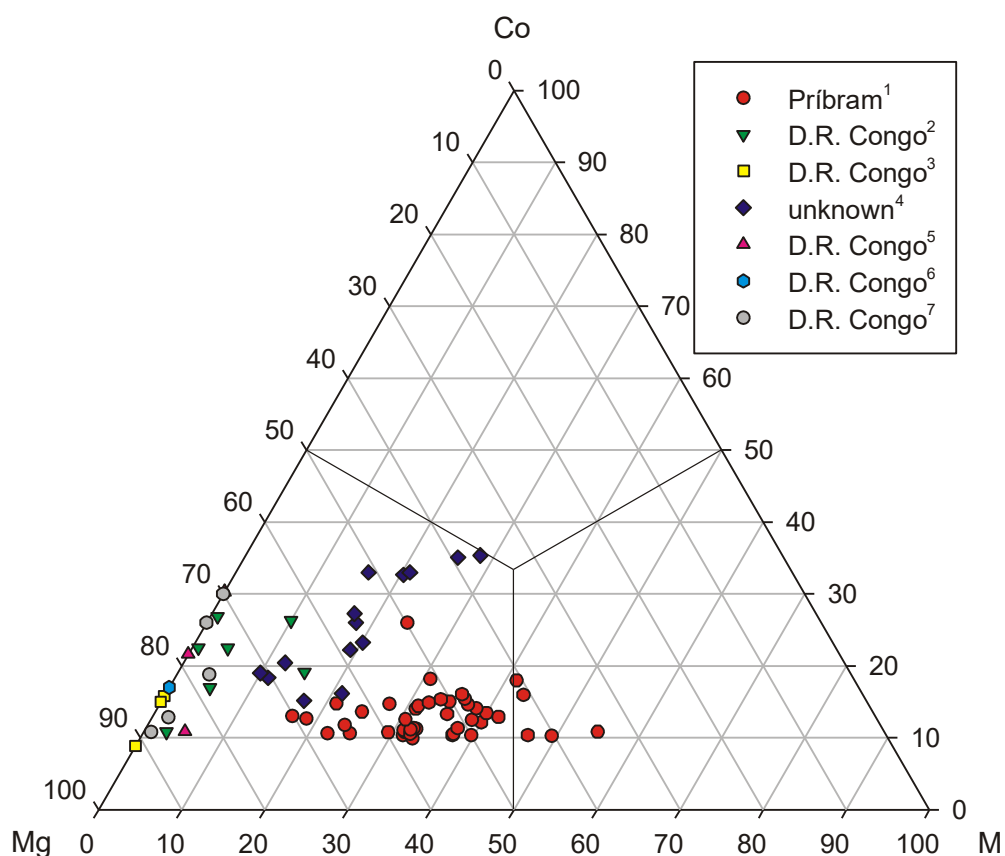


Figure 7. Chemical composition of Co-containing (with Co > 0.1 *apfu*) dolomite-group minerals in the Mg-Co-M graph (M = Fe+Mn+Zn+Cu+Ni); Příbram¹ - samples from other occurrences in the Příbram uranium district (*unpublished data of authors*), D.R. Congo² - samples from the Democratic Republic of Congo (*unpublished data of authors*), D.R. Congo³ - published data (Douglass, 1992, 1999); unknown⁴ - published data for unknown locality (Minceva-Stefanova, 1997); D.R. Congo⁵ - published data (Barton *et al.*, 2014); D.R. Congo⁶ - published data (Perchiazzi, 2015); D.R. Congo⁷ - published data (Perchiazzi *et al.*, 2018).